

Role of Porosity in Filtration IX Skin Effect with Highly Compressible Materials

FRANK M. TILLER and T. C. GREEN

Department of Chemical Engineering
University of Houston
Houston, Texas 77004

An understanding of the interplay of hydraulic pressure, compression drag pressure, flow resistance, flow rate, and porosity is essential to the field of cake filtration. Design of equipment requires a knowledge of rate of filtrate flow and average porosity as functions of applied pressure. When compressible materials exhibit rapid changes in flow resistance at low pressures, a thin skin of dry, resistant material is formed next to the media during filtration. Most of the hydraulic pressure drop is located within that narrow region. The rate of filtration can reach a maximum at relatively low pressures. Increasing pressure has little effect on reduction in average porosity, and deliquoring by direct pressure increase is ineffective. Thus filtration of such materials is best accomplished with low pressures encountered in gravity or vacuum operation.

Few authors have treated the question of porosity variation in compressible filter cakes although it is fundamental to both qualitative and quantitative problems of design and operation of solid-liquid separation equipment. Hutto (1957) and Shirato (1956) have both published data giving porosity as a function of distance through the bed. Tiller and Cooper (1962) developed analytical formulas for porosity and hydraulic pressure as a function of fractional distance for materials following modified power functions relating porosity, flow resistance, and solid compressive pressure. They provided criteria by which it was possible to classify widely divergent porosity behavior of different kinds of materials.

HYDRAULIC AND COMPRESSIVE DRAG PRESSURES

When solids are precipitated at the surface of a one-dimensional cake, the liquid flows through the interstices of the solid and exits at the other side. The hydraulic pressure p_L drops throughout the cake as the liquid flows frictionally past the individual particles. The drag imparted to the particles results in a compaction process which causes the porosity to decrease. The total drag force which is imparted from one particle to another at points of contact divided by the cross-sectional area is termed the compressive drag pressure p_s . In the normal approach to filtration theory (Tiller and Lloyd, 1972), the hydraulic and drag pressures are related by

$$p_L + p_s = p \quad (1)$$

$$dp_L + dp_s = 0 \quad (2)$$

where p may be constant or a function of time, and p_L and p_s are correspondingly functions of distance x from the media or x and t . It is assumed that the local porosity ϵ and local filtration (or flow) resistance α or permeability K are unique functions of p_s . While such an assumption has no theoretical basis, it serves as a useful approximation for developing the theory of flow through porous media.

The Shirato (Shirato et al., 1969) flow equation

$$\frac{dp_L}{dw} = \mu\alpha(q - er) \quad (3)$$

can be used in combination with Equation (2) to develop

formulas for porosity and hydraulic pressure variations. The $(q - er)$ term where q and r are respectively the superficial flow rates of liquid and solid expressed as volume/(area) (time) and e is the void ratio arises from consideration of the velocity of the liquid relative to the solid. In fixed beds, $r = 0$; and for dilute slurries (concentration of solids in slurry less than half of average concentration in cakes), it can be neglected. When r is placed equal to zero, (3) reduces to the conventional Ruth equation

$$\frac{dp_L}{dw} = -\frac{dp_s}{dw} = \mu\alpha q \quad (4)$$

or the Darcy equation

$$\frac{dp_L}{dx} = -\frac{dp_s}{dx} = \frac{1}{K} \mu q \quad (5)$$

where K is related to α by

$$K = 1/\rho_s\alpha(1 - \epsilon) \quad (6)$$

and $dw = \rho_s(1 - \epsilon) dx$

FLOW RATE VS. PRESSURE

The Darcy equation* may be rearranged in the form

$$\mu q dx = -K dp_s = -\frac{dp_s}{\rho_s\alpha(1 - \epsilon)} \quad (7)$$

where p_s is chosen for the independent variable as K , α , and ϵ are assumed to be functions of the solid compressive pressure and not p_L . Equation (7) can be integrated over a portion of the cake and then the entire cake. The limits of integration are given by

	x	p_s	p_L
Medium	0	p	0
Inside cake	x	p_s	p_L
Surface	L	0	p

where it is assumed that the medium resistance is negligible. Integrating from 0 to x and 0 to L yields (Tiller and Risbud, 1972)

$$\mu q(L - x) = \int_0^{p_s} K dp_s = \frac{1}{\rho_s} \int_0^{p_s} dp_s / \alpha(1 - \epsilon) \quad (8)$$

$$\mu qL = \int_0^p K dp_s = \frac{1}{\rho_s} \int_0^p dp_s / \alpha(1 - \epsilon) \quad (9)$$

Equation (9) provides a relationship between the flow rate, thickness L , and the pressure drop p across the cake.

If Equation (8) is divided by Equation (9) one obtains

* Equation (7) is sometimes called the Darcy-Schlichter equation. See Schlichter (1897-98).

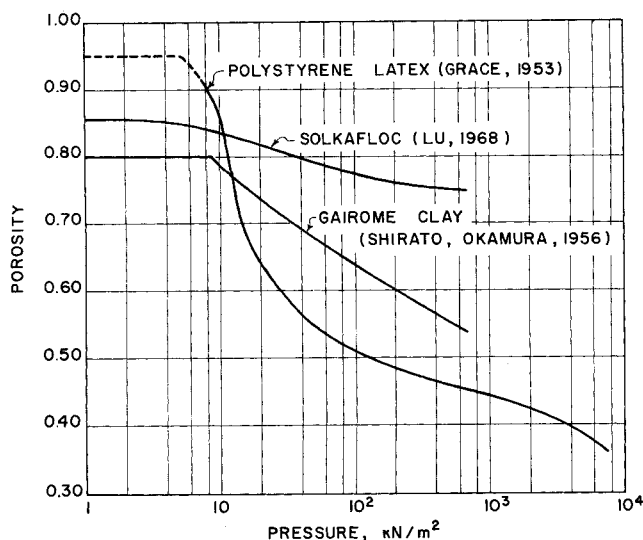


Fig. 1. Porosity vs. pressure.

$$\frac{x}{L} = \frac{\int_0^{p_s} dp_s / \alpha(1-\epsilon)}{\int_0^{p_s} dp_s / \alpha(1-\epsilon)} = \frac{\int_0^{p_s} K dp_s}{\int_0^{p_s} K dp_s} \quad (10)$$

This equation gives the fractional distance through the cake as a function of the upper limit p_s of integration. It indicates that the x/L versus p_s curves are independent of flow and total thickness. In turn, p_L (equal to $p - p_s$) and ϵ can be related to x/L through their functional relationships to p_s .

CALCULATED RESULTS

Three widely different substances (latex, Grace, 1953; Gairome clay, Shirato and Okamura 1956; solkaflocc, Nieto, 1967, and Lu, 1968) were chosen to illustrate the results which may be expected during filtration. The porosity and filtration resistance are shown in Figures 1 and 2. The resistance and porosity of the latex change radically with pressure. At high pressure, α for latex takes on values of fairly resistant materials in the neighborhood of 1-10 tera (10^{12}) filtration resistance units (m/kg) whereas solkaflocc as a filter aid assumes values one thousandth as great in the range of 1 to 10 giga (10^9) filtration resistance units. Gairome clay lies in an intermediate position.

It is virtually impossible to obtain accurate values of α and ϵ at low pressure below 5 to 10 kN/m². The dotted portions of the curves represent extrapolations of the data.

In Figure 3, plots of $1/\alpha(1-\epsilon)$ vs. p_s are shown for two of the materials. In the case of latex, the area under the curve becomes almost negligible above 10 kN/m². That behavior is a direct result of the precipitous rate of increase in the value of α in the low pressure range. As Equation (9) indicates, the flow rates are proportional to the area under the curves in Figure 3. In Figure 4, the rate-thickness product (qL) for the three materials is plotted as a function of the total pressure p . The rate-thickness product for latex rises to a maximum at a low pressure whereas it continues to increase with pressure for the solkaflocc and Gairome clay. At 10 kN/m² which is roughly equivalent to the driving force produced by a head equivalent to a meter of water, the rate-thickness product is close to its limiting value. Thus, either vacuum or gravity filtration would be indicated for latex. Pressure filtration would be the operation of choice for the Gairome

clay. The flow rates are small and increase regularly with pressure. With the solkaflocc, gravity, vacuum, or pressure could be employed. The rates are high at low pressure and increase with increasing pressure.

Analysis of the porosity and hydraulic pressure varia-

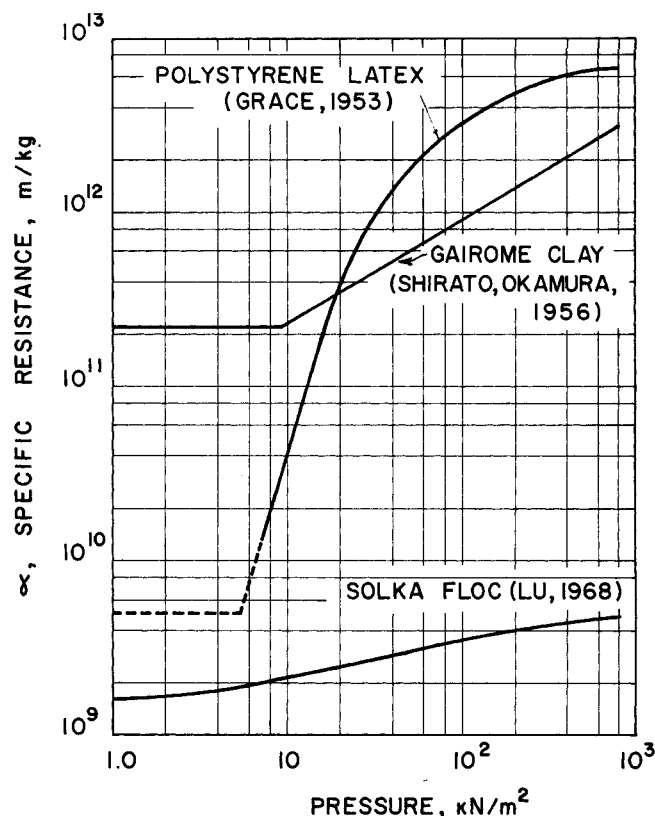


Fig. 2. Specific resistance vs. pressure.

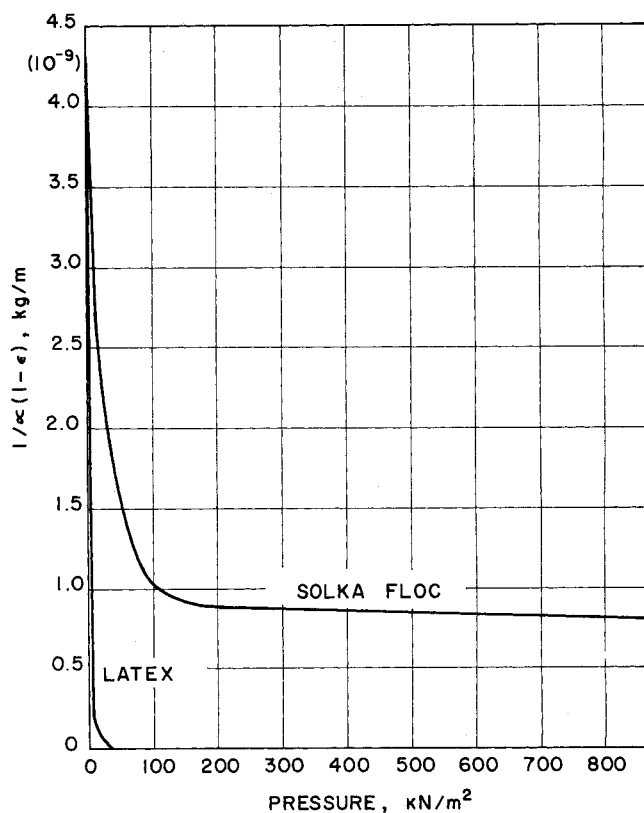


Fig. 3. Graph of $1/\alpha(1-\epsilon)$ vs. pressure.

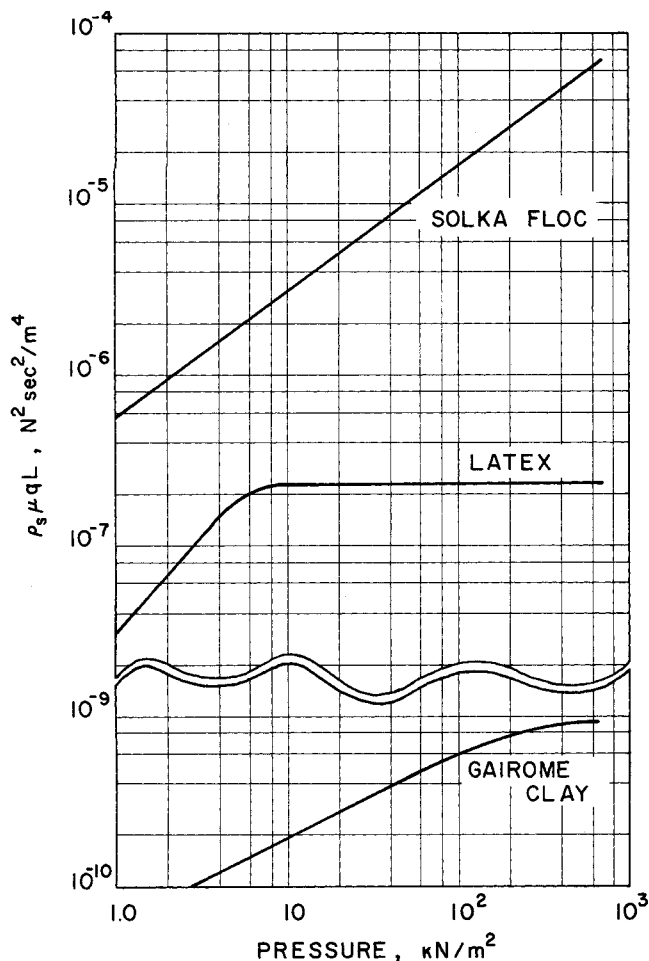


Fig. 4. Rate-thickness product vs. pressure.

compressive drag pressure. Thus the full effect of the compression is realized throughout the cake in a mechanically actuated system.

ACKNOWLEDGMENT

The authors wish to thank the National Science Foundation for support of an Undergraduate Research Participation Program which enabled T. C. Green to work in the area of filtration.

NOTATION

- e = void ratio, $\epsilon/(1 - \epsilon)$
- K = permeability, m^{-2}
- L = cake thickness, m
- p = applied pressure, N/m^2
- p_L = hydraulic pressure, N/m^2

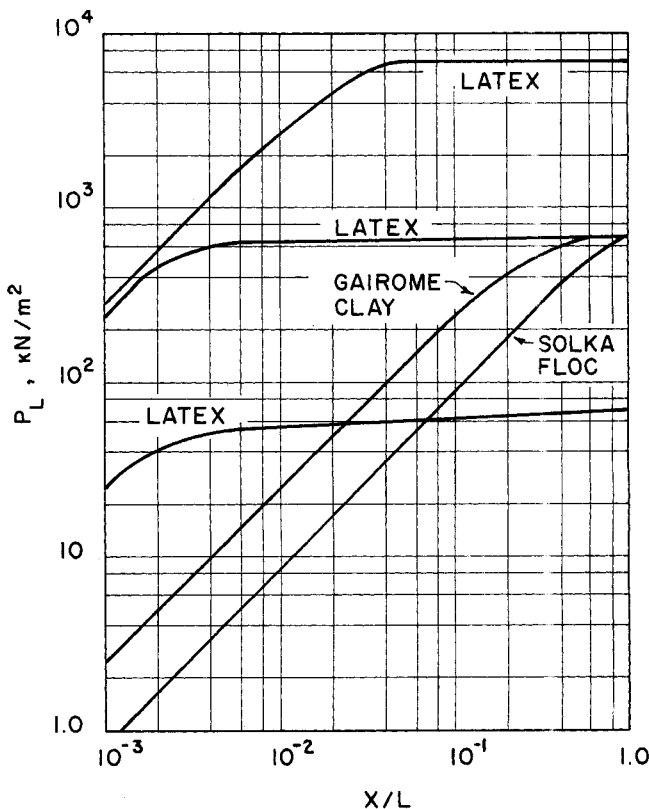


Fig. 5. Hydraulic pressure vs. fractional cake thickness.

tion with fractional distance through the cake illustrates the skin effect for latex which explains the leveling off of the rate-thickness product with increasing pressure. In Figure 5, the hydraulic pressure as calculated from Equation (10) is shown as a function of x/L . A logarithmic scale is used for x/L in order to enlarge the area of the skin effect which occurs with latex. There is very little loss in hydraulic pressure until 95 to 99% of the cake has been traversed depending upon the total pressure. With the other substances, the hydraulic pressure diminishes more uniformly throughout the cake, and there is no skin effect.

In Figure 6, the porosity is plotted against x/L . Once again the pronounced variation near the medium for the latex can be seen. In addition to adversely affecting the rate-thickness as a function of pressure, the skin effect is also deleterious to the average porosity. In many industrial filtrations, the pressure at the end of filtration is carried to a high value in order to squeeze liquid out of the cake. Although examination of the latex porosity data in Figure 2 would lead one to believe that substantial quantities of liquid could be expressed, such is not the case. Study of Figure 6 shows that the porosity is unaffected by pressure through 90% of the cake even at applied pressures as high as 7 MN/m^2 . Thus, the average porosity of the entire cake is only marginally affected by total pressure even though there is a relatively large change in the skin.

In the case of a material like latex, much better deliquoring can be accomplished by mechanical expression (Shirato et al., 1970). When a mechanical load is applied through a membrane or piston to a cake, the mechanical pressure is uniformly (except for wall friction, Tiller and Lu, 1972) distributed through the cake in contrast to the

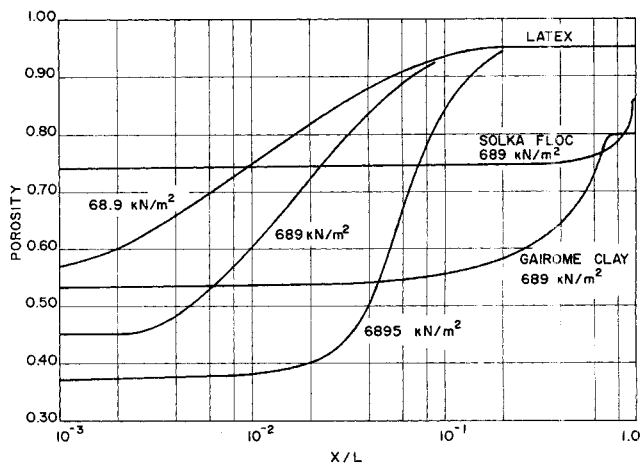


Fig. 6. Porosity vs. fractional cake thickness.

p_s = compressive drag pressure, N/m²
 q = superficial flow rate of liquid, m³/m² · s
 q_L = rate-thickness product, m²/s
 r = superficial flow rate of solids, m³/m² · s
 x = distance from medium, m
 w = mass of dry solid per unit area, kg/m²

Greek Letters

α = filtration or flow resistance, m/kg
 ϵ = porosity or volume fraction of voids, —
 μ = viscosity, N · s/m²
 ρ_s = true solid density, kg/m³

LITERATURE CITED

- Grace, H. P., "Resistance and compressibility of filter cakes," *Chem. Eng. Progr.*, **49**, 303 (1953).
- Hutto, F. B., Distribution of porosity in filter cake, *ibid.*, **53**, 328 (1957).
- Lu, Wei-Ming, "Theoretical and experimental analysis of variable pressure filtration," Ph.D. dissertation, Univ. Houston, Texas (1968).
- Nieto, Shayler, "Studies in variable pressure filtration," M.S. thesis, Univ. Houston, Texas (1967).
- Schlichter, Charles, U.S. Geol. Survey, 19th Ann. Rpt., Part II, 295-385 (1897-8).
- Shirato, M., and S. Okamura, "Behavior of Gairome clay slurries under constant pressure filtration," *Kagaku Kogaku*, **20**, 678 (1956).
- Shirato, M., M. Sambuichi, H. Kato, and T. Aragaki, "Internal flow mechanism in filter cakes," *AIChE J.*, **15**, 405 (1969).
- Shirato, M., T. Murase, M. Negawa, and T. Senda, "Fundamental studies of expression under variable pressure," *J. Chem. Eng. Japan*, **3**, 105 (1970).
- Tiller, F. M., and H. R. Cooper, "The role of porosity in filtration: part 5, porosity variation in filter cakes," *AIChE J.*, **8**, 495 (1962).
- Tiller, F. M., and P. J. Lloyd, (eds.), *Theory and practice of solid-liquid separation*, Ch. 4, Dept. of Chem. Eng., Univ. Houston, Texas (1972).
- Tiller, F. M., and Wei-Ming Lu, "The role of porosity in filtration 8; Cake non-uniformity in compression permeability cells," *AIChE J.*, **18**, 56 (1973).
- Tiller, F. M., and H. Risbud, "Hydraulic deliquoring of filter cakes, First Pacific Chemical Engineering Congress," Part 1, p. 80, *Soc. Chem. Engrs. Japan*, Amer. Inst. Chem. Engrs. (1972).

Manuscript received August 1 and accepted September 12, 1973.

Overcoming Deficiencies of the Two-Level Method for Systems Optimization

GEORGE STEPHANOPOULOS and ARTHUR W. WESTERBERG

Department of Chemical Engineering
University of Florida, Gainesville, Florida 32611

Avery and Foss (1971) have demonstrated that the method of two-level optimization (Brosilow and Lasdon, 1965; Brosilow and Nunez, 1968) may not be generally applicable to chemical process design problems due to the mathematical character of commonly encountered objective functions. The purpose of this communication is to demonstrate that this shortcoming can in fact be overcome by using a new algorithm proposed by the authors (1973).

Consider the following sequential unconstrained problem. (Constraints and recycles do not change the following results, and we want to keep the presentation here as simple as possible.)

$$\text{Min } \left\{ F|F = \sum_{i=1}^N \phi_i(x_i, u_i), x_{i+1} = f_i(x_i, u_i), \right. \\ \left. i = 1, \dots, N, x_1 = x_1^0 \text{ (given)} \right\} \quad (\text{P1})$$

The Lagrangian for this problem is

$$L = \sum_{i=1}^N \{ \phi_i(x_i, u_i) - \lambda_i^T x_i + \lambda_{i+1}^T f_i(x_i, u_i) \} \\ + \lambda_1^T x_1^0 - \lambda_{N+1}^T x_{N+1}$$

The natural boundary condition on λ_{N+1} is $\lambda_{N+1} = 0$ which yields

$$L = \sum_{i=1}^N l_i(x_i, u_i, \lambda_i, \lambda_{i+1}) + \lambda_1^T x_1^0$$

Next we define problem (P2) as

$$h(\lambda_1, \dots, \lambda_N) = \left\{ \sum_{i=1}^N \text{Min}_{x_i, u_i} l_i(x_i, u_i, \lambda_i, \lambda_{i+1}) \right\} + \lambda_1^T x_1^0 \quad (\text{P2})$$

and finally the general Lagrange problem (P3)

$$\text{Max}_{\lambda_1, \dots, \lambda_N} h(\lambda_1, \dots, \lambda_N) \quad (\text{P3})$$

The two-level method involves solving (P3) by first guessing the multipliers $\lambda_1, \dots, \lambda_N$, solving the subproblem minimizations in (P2), and then adjusting the multipliers until $h(\lambda_1, \dots, \lambda_N)$ is maximized. If the point $(\hat{x}_1, \dots, \hat{x}_N, \hat{u}_1, \dots, \hat{u}_N; \lambda_1, \dots, \lambda_N)$ is a saddle point of the Lagrangian, then the point $(\hat{x}_1, \dots, \hat{x}_N, \hat{u}_1, \dots, \hat{u}_N)$ solves problem (P1) and $(\lambda_1, \dots, \lambda_N)$ solves problem (P3).

The two-level optimization procedure fails if no saddle point exists for the Lagrangian. Avery and Foss demonstrated that in a simple heat recovery network no such saddle point can exist. Their article shows that for their problem the stationary points for the sub-Lagrangians l_i in (P2) are never at a minimum with respect to the x_i and u_i . Under these conditions the actual minimum found in (P3) will typically be at extreme values, that is, on the constraints, of the x_i and u_i variables. Usually this result precludes any chance that the equality constraints will be satisfied for (P1), and thus solving (P3) will fail to solve (P1).